



Secrecy Capacity Analysis for Indoor Visible Light Communications with Input-Dependent Gaussian Noise

Bo Huang¹  and Jianxin Dai^{2,3}  

¹ College of Telecommunications and Information Engineering, Nanjing University of Posts and Telecommunications, Nanjing 210003, China

² School of Science, Nanjing University of Posts and Telecommunications, Nanjing 210023, China
daijx@njupt.edu.cn

³ National Mobile Communications Research Laboratory, Southeast University, Nanjing 210096, China

Abstract. This paper mainly focus on the performance of secrecy capacity in the physical layer security (PLS) for the eavesdropping channel in visible light communication (VLC) system. In this system, due to the effects of thermal and shoot noises, the main interference of the channel is not only from additive white Gaussian noise (AWGN), but also dependent on the input signal. Considering a practical scenery, based on the input-dependent Gaussian noise, the closed-form expression of the upper and lower bounds of secrecy capacity are derived under the constraints of non-negative and average optical intensity. Specifically, since the entropy of the output signal is always greater than the input signal, on this basis, the derivation of lower bound is using the variational method to obtain a better input distribution. The upper bound is derived by the dual expression of channel capacity. We verified the performance of secrecy capacity through numerical results. The results show that the upper and lower bounds are relatively tight when optical intensity is high, which proves validity of the expression. In the low signal-to-noise ratio (SNR) scheme, the result of bounds with more input-dependent noise is better than less noise. And in the high SNR scheme, the result of bounds with less input-dependent noise outperforms that noise is more.

Keywords: Input-dependent Gaussian noise · Secrecy capacity · Visible light communication

1 Introduction

With the rapid progress of mobile communication technology, people have higher requirements for terminal transmission rate and security. For traditional wireless communication, there exists a series of problems, such as limited spectrum resources and easy signal fading [1]. And with the extensive use of light-emitting

diodes (LEDs) in life, visible light communication (VLC) has received more attention. In VLC system, LEDs can be used for data signal transmission while they are used for illumination [2]. LEDs have many advantageous features such as high brightness, high reliability, low power consumption and long lifespan. The VLC system consisting of LEDs has the advantages of energy saving, environmental protection, safety and reliability, and is considered as the development direction of indoor communication in the future [3].

Despite the fact that VLC has many advantages and research work on it has also been done a lot, there are still many problems to be solved for data signal transmission security. Typically, it is a challenging problem for system designers to secure the safe data signal transmission over a VLC channel in the presence of unauthorized eavesdroppers. This problem is usually solved by encryption without being considered the defects caused by the channel [4]. In this model, the primary method of secure communication is to use a secret key. Subsequently, Wyner proposed the concept of physical layer security (PLS) in his paper [5] in 1975. In [6], the secrecy capacity based on duality and multi-antenna technology in the amplitude-limited eavesdropping channel is studied. The same authors analyzed the secrecy capacity of another scenery of the free-space optical channel in [7]. On this basis, the authors in [8] studied the performance of secrecy capacity in the typical indoor eavesdropping channel under the amplitude constraints. By introducing a randomly degraded wiretap channel model, the possibility of secure communication without relying on encryption is demonstrated. The authors in [9] studied the PLS in MIMO scenery and derived the secrecy capacity and optimal deployment of the receiver. Then, the same author studied another indoor eavesdropping channel in [10] and analyzed the performance of secrecy capacity under the different optical intensity constraints, respectively. But, the noise in the channel of system model assumed by the above research work is independent additive white Gaussian noise (AWGN). In the actual VLC scenarios, since the thermal and shot noise are related to the LED illumination intensity, the noise of channel is dependent on the input signal. On this basis, Moser studied the secrecy capacity of VLC system under the input-dependent Gaussian noise in [11]. However, Moser only analyzes the situation where only legitimate receiver exists, it may also include eavesdroppers in real scenery. So the research work of secrecy capacity for eavesdropping channel is not the same.

Inspired by the previous work, this paper mainly studied the secrecy capacity of the eavesdropping channel under input-dependent Gaussian noise. Firstly, we suppose that the output signals of both legitimate receiver and eavesdropper channels are affected by input-dependent Gaussian and input-independent Gaussian noise. Under this premise, we want to secure data signal transmission for legitimate receiver and hidden information to eavesdropper. We studied the eavesdropping channel under non-negative and average optical intensity constraint and derived the upper and lower bounds of secrecy capacity on this basis.

The reminder of this paper is arranged as the follows. In Sect. 2, we describe the system and channel model. In Sect. 3, we derive the upper and lower bounds of secrecy capacity based on the information theory. We put numerical results

to compare performance of the secrecy capacity in Sect. 4. Finally, we provide concluding observations in Sect. 5.

Notations: In this paper, we use \mathbf{R} to represent the real set, and \mathbf{R}^+ is positive real set. The natural logarithm is denoted by $\ln(\cdot)$. We use $I(\cdot; \cdot)$ and $\mathcal{H}(\cdot)$ for mutual information and entropy, respectively.

2 System Model

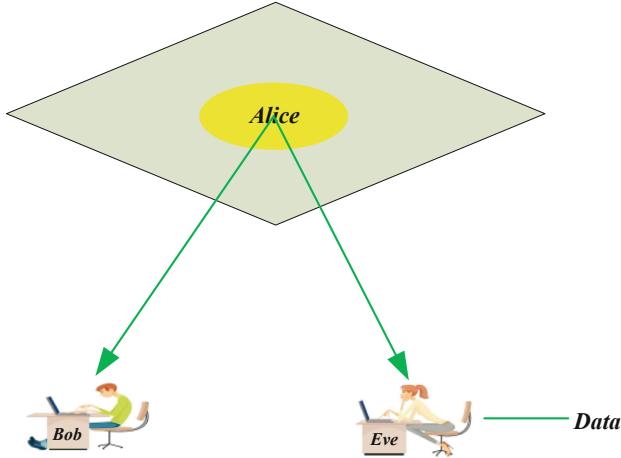


Fig. 1. An VLC network with one transmitter, one legitimate receiver and one eavesdropper.

In this paper, we consider an indoor VLC system consisting of one transmitter (Alice), one legitimate receiver (Bob), and one eavesdropper (Eve), as shown in Fig. 1. Alice acts as the transmitter to transmit data signal with one light fixture. Two receivers fixed on the desk receive the transmitted optical signal by one photodiode (PD) individually. Alice transmits data signal to Bob via VLC channel with the presence of Eve who can also receive the data signal from Alice to Bob. The received optical signals at two receivers can be mathematically expressed as [11]

$$\begin{cases} Y_B = rH_B X + \sqrt{rH_B X} Z_1 + Z_B \\ Y_E = rH_E X + \sqrt{rH_E X} Z_2 + Z_E \end{cases} \quad (1)$$

where the X is the input optical signal and is non-negative, H_B and H_E are the channel gains representing Bob and Eve, respectively. r indicates the photoelectric conversion coefficient whose value is generally set to one. Y_B and Y_E are the received signals of Bob and Eve, respectively. $Z_B \in N(0, \sigma_B^2)$ and $Z_E \in N(0, \sigma_E^2)$ are independent AWGN, $Z_1 \in N(0, \varsigma_1^2 \sigma_B^2)$ and $Z_2 \in N(0, \varsigma_1^2 \sigma_E^2)$ are input-dependent AWGN. We assume that Z_B , Z_E , Z_1 and Z_2 are irrelevant. ς_1^2 and

ς_2^2 represent the ratio of Bob and Eve's input-dependent Gaussian noise and input-independent noise variance, respectively.

The conditional probability density function (PDF) of eavesdropping channel can be expressed as [11]

$$\begin{cases} f_{Y_B|X}(y_B|x) = \frac{1}{\sqrt{2\pi(1+H_B x \varsigma_1^2)}\sigma_B^2} e^{-\frac{(y_B-H_B x)^2}{2(1+H_B x \varsigma_1^2)\sigma_B^2}} \\ f_{Y_E|X}(y_E|x) = \frac{1}{\sqrt{2\pi(1+H_E x \varsigma_2^2)}\sigma_E^2} e^{-\frac{(y_E-H_E x)^2}{2(1+H_E x \varsigma_2^2)\sigma_E^2}} \end{cases} \quad (2)$$

Furthermore, we assume $f_X(x)$ is the input PDF, and $f_{Y_B}(y_B)$ and $f_{Y_E}(y_E)$ are the output PDFs respectively. Due to that intensity modulation at the transmitter and direct detection at the receiver in the VLC, input signal X is limited to non-negative

$$X \geq 0 \quad (3)$$

Since indoor VLC also ensures illumination while transmitting data signals, the average optical intensity should be limited as follows

$$E(X) = \xi P \quad (4)$$

where $\xi \in (0, 1]$ is the dimming target, and $P > 0$ is the general optical intensity level of LEDs. In the indoor VLC scenery, channel gain H_k ($k = B, E$) can be mathematically expressed as [10]

$$H_k = \begin{cases} \frac{(m+1)A_r}{2\pi D_k^2} T_s g \cos^m(\varphi_k) \cos(\psi_k), & \text{if } 0 \leq \psi_k \leq \Psi \\ 0, & \text{if } \psi_k \geq \Psi \end{cases} \quad (5)$$

where m is the order of the Lambertian emission, A_r is the physical area of the PD, T_s and g are the optical filter gain and the concentrator gain of the PD, respectively. Ψ is the field of view (FOV) of the PD. D_k , φ_k and ψ_k are the distance, the angle of irradiance and the angle of incidence between LED and PD.

3 Secrecy Capacity Analysis

In this section, we mainly analyze the secrecy capacity in VLC system of an input-dependent Gaussian noise under average optical intensity constraint. When the channel of Bob is worse than the Eve, i.e., $H_B/\sigma_B < H_E/\sigma_E$, the channel Bob is stochastically faded with regarding to the channel of Alice-Eve, and the value of the secrecy capacity is near zero. Conversely, when the channel of Bob is better than the channel of Eve, i.e., $H_B/\sigma_B \geq H_E/\sigma_E$, the secrecy capacity can be expressed as [8]

$$\begin{aligned} C_s &= \max_{f_X(x)} [I(X; Y_B) - I(X; Y_E)] \\ \text{s.t. } &\int_0^\infty f_X(x) dx = 1 \\ &E(X) = \int_0^\infty x f_X(x) dx = \xi P \end{aligned} \quad (6)$$

where C_s indicates the secrecy capacity and $f_X(x)$ represents the PDF of input data signal. The upper and lower bounds of secrecy capacity will be derived in this part. Based on this analysis, the security performance is analyzed.

3.1 Lower Bound Analysis

For any two arbitrary functions $f_1(x)$ and $f_2(x)$, there exists the inequality $\max_x (f_1(x) - f_2(x)) \geq \max_x f_1(x) - \max_x f_2(x)$ [11]. Therefore, the secrecy capacity in (6) can be lower-bounded as following

$$\begin{aligned} C_s &\geq \max_{f_X(x)} I(X; Y_B) - \max_{f_X(x)} I(X; Y_E) \\ &\geq I(X; Y_B) - I(X; Y_E)|_{any f_X(x)} \\ &= \mathcal{H}(Y_B) - \mathcal{H}(Y_B|X) - \mathcal{H}(Y_E) + \mathcal{H}(Y_E|X) \end{aligned} \quad (7)$$

where $\mathcal{H}(\cdot)$ denotes entropy. By using the entropy power inequality (EPI) and variational method, we derived the expression of lower bound of secrecy capacity according to the theorem as follows.

Theorem 1. *The secrecy capacity of input-dependent Gaussian noise channel with the input signal satisfies the constraints (3) and (4) is lower-bounded by*

$$\begin{aligned} C_s &\geq \sqrt{\frac{6}{\pi\xi P}} - \ln \left[\frac{3\sqrt{3}}{\sqrt{2\pi}(\xi P)^{\frac{3}{2}}} \right] + \frac{1}{2} \ln \left(H_B + \frac{2\varsigma_1^2 \sigma_B^2}{\xi P} \right) - 1 - \frac{\xi P}{\varsigma_1^2 \sigma_B^2} \\ &\quad - \frac{1}{2} \ln \left\{ 2\pi e \left[\frac{2}{3} H_E^2 \xi^2 P^2 + \frac{16}{\sqrt{2\pi}} H_E \xi P \varsigma_2^5 \sigma_E^5 + \sigma_E^2 \right] \right\} \\ &\quad + \frac{\sqrt{\xi P (H_B \xi P + 2\varsigma_1^2 \sigma_B^2)}}{\varsigma_1^2 \sigma_B^2} + \frac{1}{2} \ln \left(\frac{\sigma_E^2}{\sigma_B^2} \right) + \frac{\varsigma_2^2}{2\varsigma_1^2} \end{aligned} \quad (8)$$

Proof. See Appendix A.

3.2 Upper Bound Analysis

The dual expression based on mutual information in [6] gave an analysis of the upper bound of the secrecy capacity. The method is effective for solving the upper bound of secrecy capacity on the general eavesdropping channel, and the method will also be cited in this paper.

Proposition 1. Consider a VLC channel $f(\cdot|\cdot)$ with input as $X \in \mathbf{R}^+$, and output as $Y \in \mathbf{R}$. For any one of the output distributions $Y(\cdot)$, we have

$$C \leq E_{f_X^*} (D(f_{\cdot|X}(\cdot|x) || Y(\cdot))) \quad (9)$$

where the $D(\cdot||\cdot)$ denotes relative entropy [12], $f_X^*(x)$ denotes the capacity-achieving distribution of input signal.

Based on the above ideas, the upper bound of the secrecy capacity can be derived. It is known from Proposition 1, an upper bound of secrecy capacity can be obtained for any distribution of output signal. Our goal is to choose a better distribution that makes the upper bound more closer to the lower bound. As for any PDF $g_{Y_B|Y_E}(y_B|y_E)$, we have [13]

$$\begin{aligned} & I(X; Y_B|Y_E) + E_{X Y_E} \left\{ D(f_{Y_B|Y_E}(y_B|Y_E) \parallel g_{Y_B|Y_E}(y_B|Y_E)) \right\} \\ &= E_{X Y_E} \left\{ D(f_{Y_B|X Y_E}(y_B|X, Y_E) \parallel g_{Y_B|Y_E}(y_B|Y_E)) \right\} \end{aligned} \quad (10)$$

According to non-negative properties based relative entropy, we have

$$I(X; Y_B|Y_E) \leq E_{X Y_E} \left\{ D(f_{Y_B|X Y_E}(y_B|X, Y_E) \parallel g_{Y_B|Y_E}(y_B|Y_E)) \right\} \quad (11)$$

Noted that, the upper bound of $I(X; Y_B|Y_E)$ can be derived for any PDF $g_{Y_B|Y_E}(y_B|y_E)$.

$$I(X; Y_B|Y_E) = \min_{g_{Y_B|Y_E}(y_B|y_E)} E_{X Y_E} \left\{ D(f_{Y_B|X Y_E}(y_B|X, Y_E) \parallel g_{Y_B|Y_E}(y_B|Y_E)) \right\} \quad (12)$$

It's clear that, in order to obtain secrecy capacity, there exists an input distribution to maximize the $I(X; Y_B|Y_E)$ satisfying the constraint in (6). Therefore, we have

$$\begin{aligned} C_s &= \max_{f_X(x)} I(X; Y_B|Y_E) \\ &= I(X^*; Y_B|Y_E) \end{aligned} \quad (13)$$

where X^* denotes the optimal distribution of input signal, the corresponding PDF is $f_{X^*}(x)$. According to (3.2) and (13), we have

$$C_s \leq E_{X^* Y_E} \left\{ D(f_{Y_B|X Y_E}(y_B|X, Y_E) \parallel g_{Y_B|Y_E}(y_B|Y_E)) \right\} \quad (14)$$

It can be seen from (14) that the choice of any $g_{Y_B|Y_E}(y_B|y_E)$ will cause the upper bound. In order to get a better result, we should find a better choice of $g_{Y_B|Y_E}(y_B|y_E)$. By using dual expression, the upper bound in (6) can be given by the theorem as follows.

Theorem 2. *The secrecy capacity of input-dependent Gaussian noise channel in (1) under the constraints (3) and (4) is upper bounded by*

$$C_s \leq \begin{cases} I_1 + \ln \left[4e \left(\sqrt{\frac{3}{\pi^2 H_B^2 \sigma_1^2 \sigma_B^2 \epsilon^2 P} + \frac{H_B \epsilon P}{2}} \right) \right], & \text{if } \sqrt{\frac{3}{\pi^2 \xi P \left(\frac{H_E^2}{H_B^2} \sigma_1^2 \sigma_B^2 + H_{E\sigma}^2 \sigma_E^2 \right)}} \geq \frac{H_E}{H_B} \left(\sqrt{\frac{3}{\pi^2 H_B^2 \sigma_1^2 \sigma_B^2 \epsilon^2 P} + \frac{H_B \epsilon P}{2}} \right) \\ I_1 + \ln \left[4e \frac{H_B}{H_E} \sqrt{\frac{3}{\pi^2 \xi P \left(\frac{H_E^2}{H_B^2} \sigma_1^2 \sigma_B^2 + H_{E\sigma}^2 \sigma_E^2 \right)}} \right], & \text{if } \sqrt{\frac{3}{\pi^2 \xi P \left(\frac{H_E^2}{H_B^2} \sigma_1^2 \sigma_B^2 + H_{E\sigma}^2 \sigma_E^2 \right)}} < \frac{H_E}{H_B} \left(\sqrt{\frac{3}{\pi^2 H_B^2 \sigma_1^2 \sigma_B^2 \epsilon^2 P} + \frac{H_B \epsilon P}{2}} \right) \end{cases} \quad (15)$$

where I_1 can be written as

$$\begin{aligned}
 I_1 = & \frac{1}{2} + \frac{1}{\sqrt{\pi}} - \frac{\sqrt{2}}{2} + \ln\left(\frac{\sigma_E}{\sigma_B}\right) \\
 & - \frac{\varsigma_2^2}{2\varsigma_1^2} - \frac{\ln(2\pi)}{\sqrt{\pi}} - \left(\frac{1}{\sqrt{\pi}} + \frac{\sqrt{2}}{2}\right) \left(\frac{H_E^2}{H_B^2}\sigma_B^2 + \sigma_E^2\right) \\
 & - \xi P \left(\frac{1}{2} + \frac{\sqrt{2\pi}}{4}\right) \left(\frac{H_E^2}{H_B^2}H_B\varsigma_1^2\sigma_B^2 + H_E\varsigma_2^2\sigma_E^2\right)
 \end{aligned} \tag{16}$$

Proof. See Appendix B.

4 Numerical Results

In this section, we consider a typical indoor VLC network scenery in a $10 \times 10 \times 5 \text{ m}^3$ conference room. Room lighting is provided by one LED that emits the optical power signal. Alice is placed in the center of the ceiling and modulated to transmit data signals. Bob and Eve are placed at the height of 0.9 meters above the ground. Other parameters for simulation are shown in Table 1.

Table 1. Main simulation parameters

Parameter	Value
Order of the Lambertian emission m	6
Physical area of the PD A_r	1 cm ²
Optical filter gain T_s	1
Concentrator gain g	3
Noise variance $\sigma^2 = \sigma_B^2 = \sigma_E^2$	-120 dBm
FOV of PD	70 ⁰
Position of Bob	(0 m, 0 m, 0.9 m)
Position of Eve	(2.57 m, -3.86 m, 0.9 m)

In Fig. 2, we assume that the dimming target is $\xi = 0.3$, giving the gap between the upper and lower bounds under different ς_1/ς_2 . It can be seen from the figure that when P is small (i.e., the low SNR scheme), the upper and lower bounds increase with the increase of P ; when P is larger (i.e., the high SNR scheme), the upper and lower bounds tend to be constant as the P grows. With the decrease of ς_1/ς_2 , the upper and lower bounds are more tighter. The gap between the upper and lower bounds of the secrecy capacity is smaller when P is larger. At a low SNR scheme, the performance of bound with high value ς_1/ς_2 outperforms that with low value ς_1/ς_2 . At a high SNR scheme, the bounds of secrecy capacity performance become better as the ς_1/ς_2 is big.

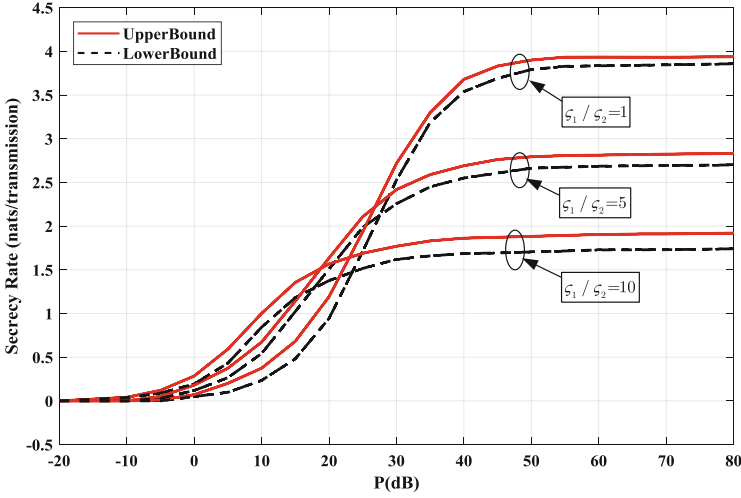


Fig. 2. Secrecy capacity under the different ς_1/ς_2 while the dimming target is $\xi = 0.3$.

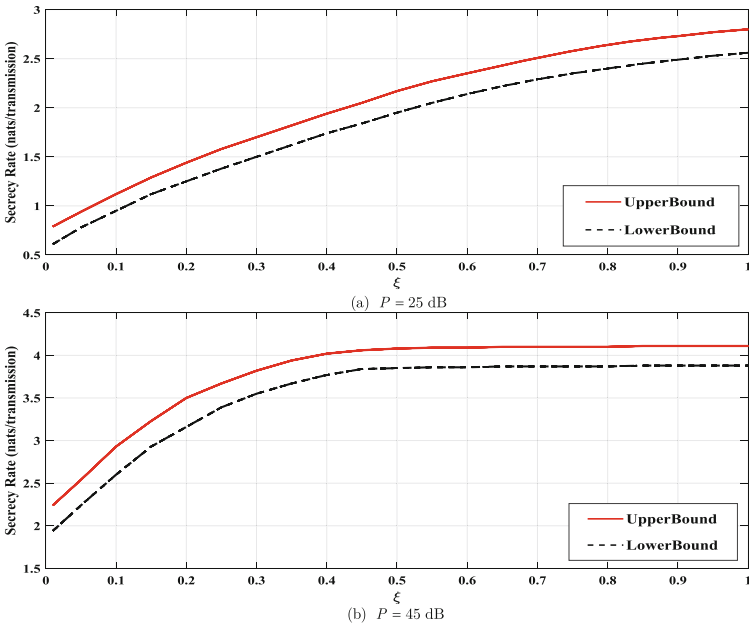


Fig. 3. Secrecy capacity under the different diming target ξ while the $\varsigma_1/\varsigma_2 = 1$.

It can be seen from Fig. 3 that, the upper and lower bounds of the secrecy capacity increase with increase of ξ when P is small. When P grows to a certain value, the bounds of secrecy capacity tends to be constant while ξ is larger. And when P is larger, the upper and lower bounds stays unchanged with the increase of ξ .

5 Conclusion

In this paper, we analyzed the secrecy capacity of VLC system with input-dependent Gaussian noise channel in typical indoor scenery. Under the constraint of average optical intensity, the closed-form expression of the upper and lower bounds of the secrecy capacity are derived. The numerical results show that the gap between the upper and lower bounds is smaller when SNR is high. The input-dependent Gaussian noise work done in this paper is a supplement to the previous research of VLC system. The channel model considered in previous works can be regarded as a special case of this paper (i.e., $\varsigma_1 = \varsigma_2 = 0$).

6 Appendix

6.1 Appendix A

For expression (7), according to [10], we have

$$\begin{aligned} \mathcal{H}(Y_B) &\geq \mathcal{H}(H_B X) + f_{\text{low}}(\xi P) \\ &= \mathcal{H}(X) + \ln(H_B) + f_{\text{low}}(\xi P) \end{aligned} \quad (17)$$

According to Theorem 17.2.3 in [12], an upper bound of $\mathcal{H}(Y_E)$ is given by

$$\mathcal{H}(Y_E) \leq \frac{1}{2} \ln [2\pi e \text{var}(Y_E)] \quad (18)$$

Substituting (17) and (18) into (7), C_s can be written as

$$C_s \geq \mathcal{H}(X) + \ln(H_B) + f_{\text{low}}(\xi P) - \mathcal{H}(Y_B | X) - \frac{1}{2} \ln [2\pi e \text{var}(Y_E)] + \mathcal{H}(Y_E | X) \quad (19)$$

where $f_{\text{low}}(\xi P)$, $\mathcal{H}(Y_B | X)$ and $\mathcal{H}(Y_E | X)$ are given by

$$f_{\text{low}}(\xi P) = \frac{1}{2} \ln \left(H_B + \frac{2\varsigma_1^2 \sigma_B^2}{\xi P} \right) - \frac{\xi P + \varsigma_1^2 \sigma_B^2}{\varsigma_1^2 \sigma_B^2} + \frac{\sqrt{\xi P (H_B \xi P + 2\varsigma_1^2 \sigma_B^2)}}{\varsigma_1^2 \sigma_B^2} \quad (20)$$

$$\begin{aligned} \mathcal{H}(Y_B | X) &= \frac{1}{2} E_{f_X} \{ \ln [2\pi e \sigma_B^2 (1 + \varsigma_1^2 X)] \} \\ &= \frac{1}{2} \ln (2\pi e \sigma_B^2) + \frac{1}{2} E_{f_X} [\ln (1 + \varsigma_1^2 X)] \end{aligned} \quad (21)$$

$$\mathcal{H}(Y_E | X) = \frac{1}{2} \ln (2\pi e \sigma_E^2) + \frac{1}{2} E_{f_X} [\ln (1 + \varsigma_2^2 X)] \quad (22)$$

Then C_s in (19) can be written as

$$\begin{aligned} C_s &\geq \mathcal{H}(X) + \frac{1}{2} \ln \left(H_B + \frac{2\varsigma_1^2 \sigma_B^2}{\xi P} \right) - \frac{\xi P + \varsigma_1^2 \sigma_B^2}{\varsigma_1^2 \sigma_B^2} \\ &\quad + \frac{\sqrt{\xi P (H_B \xi P + 2\varsigma_1^2 \sigma_B^2)}}{\varsigma_1^2 \sigma_B^2} - \frac{1}{2} \ln [2\pi e \text{var}(Y_E)] + \frac{1}{2} \ln \left(\frac{\sigma_E^2}{\sigma_B^2} \right) \\ &\quad + \frac{1}{2} E_{f_X} \{ \ln(X) \} + \frac{1}{2} E_{f_X} \left\{ \ln \left(\frac{1 + \varsigma_2^2 X}{X + \varsigma_1^2 X^2} \right) \right\} \end{aligned} \quad (23)$$

where the $E_{f_X} \{ \ln [(1 + \varsigma_2^2 X)/(X + \varsigma_1^2 X^2)] \}$ is tends to zero when X is infinite.

We select an input distribution $f_X(x)$ to maximize the $\mathcal{H}(X)+1/2\{E_{f_X}[\ln(X)]\}$ under the input constraints (3) and (4). Such an optimization problem as following can be solved to find the better input PDF.

$$\begin{aligned} & \max_{f_X(x)} \left\{ \mathcal{H}(X) + \frac{1}{2} E_{f_X} [\ln(X)] \right\} \\ & \text{s.t.} \quad \int_0^\infty f_X(x) dx = 1 \\ & \quad \quad E(X) = \int_0^\infty x f_X(x) dx = \xi P \end{aligned} \quad (24)$$

Then an optimal distribution problem can be transformed as

$$\begin{aligned} & \max_{f_X(x)} F[f_X(x)] \triangleq \int_0^\infty \left\{ \frac{1}{2} \ln(x) - \ln[f_X(x)] \right\} f_X(x) dx \\ & \text{s.t.} \quad \int_0^\infty f_X(x) dx = 1 \\ & \quad \quad E(X) = \int_0^\infty x f_X(x) dx = \xi P \end{aligned} \quad (25)$$

This problem can be solved by variational method. Assuming that optimal result in (24) is $f_X(x)$, then define a perturbation function as

$$\tilde{f}_X(x) = f_X(x) + \varepsilon \eta(x) \quad (26)$$

where ε is a variable, and $\eta(x)$ is a function, where x is the independent variable of the function. And the perturbation function in (26) should also satisfy the constraints in (24). So we have

$$\begin{cases} \int_0^\infty \eta(x) dx = 0 \\ \int_0^\infty x \eta(x) dx = 0 \end{cases} \quad (27)$$

Then define a function $\rho(\varepsilon)$, where ε is the independent variable of the function.

$$\rho(\varepsilon) = F[\tilde{f}_X(x)] = F[f_X(x) + \varepsilon \eta(x)] \quad (28)$$

The extremum value is obtained when $\varepsilon = 0$, the first variation can be expressed as

$$\left. \frac{d\rho(\varepsilon)}{d\varepsilon} \right|_{\varepsilon=0} = \int_0^\infty \left\{ \frac{1}{2} \ln(x) - \ln[f_X(x)] - 1 \right\} \eta(x) dx = 0 \quad (29)$$

So we have

$$f_X(x) = \sqrt{x} e^{-cx-b} \quad (30)$$

where b and c are the free parameters. Submitting (30) into the constraints in (25), we have

$$\begin{cases} b = \ln \left[\frac{\sqrt{2\pi}(\xi P)^{\frac{3}{2}}}{3\sqrt{3}} \right] \\ c = \frac{3}{2\xi P} \end{cases} \quad (31)$$

And $f_X(x)$ in (30) can be written as

$$f_X(x) = \frac{3}{\xi P} \sqrt{\frac{3}{2\pi\xi P}} \sqrt{x} e^{-\frac{3}{2\xi P}x} \quad (32)$$

The unknowns $\mathcal{H}(X)$, $\frac{1}{2}E_{f_X}\{\ln(X)\}$ and $\frac{1}{2}E_{f_X}\{\ln[(1+\varsigma_2^2X)/(X+\varsigma_1^2X^2)]\}$ in (23) can be solved as following

$$\begin{aligned} \mathcal{H}(X) &= -\int_0^\infty f_X(x) \ln[f_X(x)] dx \\ &= -\frac{3\sqrt{3}}{\sqrt{2\pi}(\xi P)^{\frac{3}{2}}} \left\{ \ln \left[\frac{3\sqrt{3}}{\sqrt{2\pi}(\xi P)^{\frac{3}{2}}} \right] \int_0^\infty \sqrt{x} e^{-\frac{3}{2\xi P}x} dx \right. \\ &\quad \left. + \frac{1}{2} \int_0^\infty \sqrt{x} e^{-\frac{3}{2\xi P}x} \ln(x) dx - \frac{3}{2\xi P} \int_0^\infty \sqrt{x} e^{-\frac{3}{2\xi P}x} x dx \right\} \\ &\leq \frac{1}{2} + \sqrt{\frac{6}{\pi\xi P}} - \ln \left[\frac{3\sqrt{3}}{\sqrt{2\pi}(\xi P)^{\frac{3}{2}}} \right] \end{aligned} \quad (33)$$

$$\begin{aligned} &\frac{1}{2}E_{f_X}\{\ln(X)\} + \frac{1}{2}E_{f_X}\left\{\ln\left(\frac{1+\varsigma_2^2X}{X+\varsigma_1^2X^2}\right)\right\} \\ &= \frac{1}{2}E_{f_X}\left\{\ln\left(\frac{1+\varsigma_2^2X}{1+\varsigma_1^2X}\right)\right\} \\ &\leq \frac{1}{2} \int_0^\infty \frac{3\sqrt{3}}{\sqrt{2\pi}(\xi P)^{\frac{3}{2}}} \sqrt{x} e^{-\frac{3}{2\xi P}x} \left(\frac{1+\varsigma_2^2x}{1+\varsigma_1^2x} - 1\right) dx \\ &= \frac{1}{2} \left(\frac{\varsigma_2^2}{\varsigma_1^2} - 1\right) \text{erfc}(0) = \frac{\varsigma_2^2}{2\varsigma_1^2} - \frac{1}{2} \end{aligned} \quad (34)$$

As for $\text{var}(Y_E)$, we have

$$\begin{aligned} \text{var}(Y_E) &= \text{var}(H_E X) + \text{var}\left(\sqrt{H_E X} Z_2\right) + \text{var}(Z_E) \\ &= H_E^2 \text{var}(X) + H_E \text{var}\left(\sqrt{X} Z_2\right) + \text{var}(Z_E) \end{aligned} \quad (35)$$

The $\text{var}(X)$ and $\text{var}\left(\sqrt{X} Z_2\right)$ can be written as

$$\text{var}(X) = E(X^2) - [E(X)]^2 = \frac{2}{3}\xi^2 P^2 \quad (36)$$

$$\text{var}\left(\sqrt{X} Z_2\right) = E\left[\left(\sqrt{X}\right)^2 Z_2^2\right] - \left[E\left(\sqrt{X} Z_2\right)\right]^2 = \frac{16}{\sqrt{2\pi}} \xi P \varsigma_2^5 \sigma_E^5 \quad (37)$$

Submitting (36) and (37) into (35), we have

$$\text{var}(Y_E) = \frac{2}{3} H_E^2 \xi^2 P^2 + \frac{16}{\sqrt{2\pi}} H_E \xi P \varsigma_2^5 \sigma_E^5 + \sigma_E^2 \quad (38)$$

Then substituting (33), (34) and (38) into (23), (8) can be derived.

6.2 Appendix B

Expression (14) can be written as

$$C_s \leq E_{X^*} \left\{ \underbrace{\int_{-\infty}^{\infty} \int_{-\infty}^{\infty} f_{Y_B Y_E | X} (y_B, y_E | X) \ln [f_{Y_B | X Y_E} (y_B | X, y_E)] dy_B dy_E}_{I_1} \right. \\ \left. - E_{X^*} \left\{ \underbrace{\int_{-\infty}^{\infty} \int_{-\infty}^{\infty} f_{Y_B Y_E | X} (y_B, y_E | X) \ln [g_{Y_B | Y_E} (y_B | y_E)] dy_B dy_E}_{I_2} \right\} \right\} \quad (39)$$

I_1 can be written as

$$I_1 = E_{X^*} \left\{ \int_{-\infty}^{\infty} \int_{-\infty}^{\infty} f_{Y_B | X Y_E} (y_B | X, y_E) \ln [f_{Y_B | X Y_E} (y_B | X, y_E)] dy_B dy_E \right\} \\ = -\mathcal{H}(Y_B | X^*, Y_E) \\ = -[\mathcal{H}(Y_B | X^*) + \mathcal{H}(Y_E | X^*, Y_B) - \mathcal{H}(Y_E | X^*)] \quad (40)$$

Obtained by (21) and (22), $\mathcal{H}(Y_B | X^*)$ and $\mathcal{H}(Y_E | X^*)$ can be written as

$$\begin{cases} \mathcal{H}(Y_B | X^*) = H(Y_B | X) = \frac{1}{2} \ln(2\pi e \sigma_B^2) + \frac{1}{2} E_{f_X} [\ln(1 + \varsigma_1^2 X)] \\ \mathcal{H}(Y_E | X^*) = H(Y_E | X) = \frac{1}{2} \ln(2\pi e \sigma_E^2) + \frac{1}{2} E_{f_X} [\ln(1 + \varsigma_2^2 X)] \end{cases} \quad (41)$$

As for $H(Y_E | X^*, Y_B)$, the conditional PDF $f_{Y_E | Y_B}(y_E | y_B)$ can be expressed as

$$f_{Y_E | Y_B}(y_E | y_B) = \frac{1}{\sqrt{2\pi \left[\left(\frac{H_E^2}{H_B^2} + \frac{H_E^2}{H_B^2} \varsigma_1^2 \right) \sigma_B^2 + (1 + H_E \varsigma_2^2) \sigma_E^2 \right]}} e^{-\frac{\left(y_E - \frac{H_E}{H_B} y_B \right)^2}{2 \left[\left(\frac{H_E^2}{H_B^2} + \frac{H_E^2}{H_B^2} \varsigma_1^2 \right) \sigma_B^2 + (1 + H_E \varsigma_2^2) \sigma_E^2 \right]}} \quad (42)$$

$\mathcal{H}(Y_E | X^*, Y_B)$ can be expressed as

$$\mathcal{H}(Y_E | X^*, Y_B) = -\int_0^{\infty} f_{X^*}(x) \int_{-\infty}^{\infty} f_{Y_B | X^*}(y_B | x) \int_{-\infty}^{\infty} f_{Y_E | Y_B}(y_E | y_B) \ln f_{Y_E | Y_B}(y_E | y_B) dy_B dy_E dx \\ = \frac{3\sqrt{3}}{2\sqrt{2\pi}(\xi P)^{\frac{3}{2}}} \left\{ \ln(2\pi) \int_0^{\infty} \sqrt{x} e^{-\frac{3}{2\xi P}x} dx \right. \\ \left. + \int_0^{\infty} \sqrt{x} e^{-\frac{3}{2\xi P}x} \ln \left[\left(\frac{H_E^2}{H_B^2} + \frac{H_E^2}{H_B^2} \varsigma_1^2 \right) \sigma_B^2 + (1 + H_E \varsigma_2^2) \sigma_E^2 \right] dx \right. \\ \left. + \sqrt{2\pi} \int_0^{\infty} \sqrt{x} e^{-\frac{3}{2\xi P}x} \sqrt{\left(\frac{H_E^2}{H_B^2} + \frac{H_E^2}{H_B^2} \varsigma_1^2 \right) \sigma_B^2 + (1 + H_E \varsigma_2^2) \sigma_E^2} dx \right\} \\ \geq \frac{1}{\sqrt{\pi}} [\ln(2\pi) - 2] + \left(\frac{1}{\sqrt{\pi}} + \frac{\sqrt{2}}{2} \right) \left(\frac{H_E^2}{H_B^2} \sigma_B^2 + \sigma_E^2 + 1 \right) \\ + \left(\frac{\xi P}{2} + \frac{\sqrt{2\pi}\xi P}{4} \right) \left(\frac{H_E^2}{H_B^2} \varsigma_1^2 \sigma_B^2 + H_E \varsigma_2^2 \sigma_E^2 \right) \quad (43)$$

Substituting (43) and (41) into (40), we have

$$\begin{aligned}
 I_1 \leq & \frac{1}{2} + \frac{1}{\sqrt{\pi}} - \frac{\sqrt{2}}{2} + \ln \left(\frac{\sigma_E}{\sigma_B} \right) - \frac{\varsigma_2^2}{2\varsigma_1^2} \\
 & - \frac{\ln(2\pi)}{\sqrt{\pi}} - \left(\frac{1}{\sqrt{\pi}} + \frac{\sqrt{2}}{2} \right) \left(\frac{H_E^2}{H_B^2} \sigma_B^2 + \sigma_E^2 \right) \\
 & - \xi P \left(\frac{1}{2} + \frac{\sqrt{2\pi}}{4} \right) \left(\frac{H_E^2}{H_B^2} H_B \varsigma_1^2 \sigma_B^2 + H_E \varsigma_2^2 \sigma_E^2 \right)
 \end{aligned} \tag{44}$$

One of the difficulties in solving I_2 is that the input signal X has no peak intensity constraints so it is difficult to find the bounds of upper bound because the signal range can be arbitrarily large. In order to get I_2 , $g_{Y_B|Y_E}(y_B|y_E)$ can be chosen as [10]

$$g_{Y_B|Y_E}(y_B|y_E) = \frac{1}{2s^2} e^{-\frac{|y_B - \mu y_E|}{s^2}} \tag{45}$$

where s and μ are free parameters.

Let $p = [H_E^2/H_B^2 + (H_E^2/H_B) x \varsigma_1^2] \sigma_B^2 + (1 + H_E x \varsigma_2^2) \sigma_E^2$ and $q = (1 + H_B x \varsigma_1^2) \sigma_B^2$. Therefore, $f_{Y_B Y_E|X}(y_B, y_E|X)$ can be written as

$$f_{Y_B Y_E|X}(y_B, y_E|X) = \frac{1}{\sqrt{2\pi q}} e^{-\frac{(y_B - H_B x)^2}{2q}} \times \frac{1}{\sqrt{2\pi p}} e^{-\frac{(y_E - \frac{H_E}{H_B} y_B)^2}{2p}} \tag{46}$$

Substituting (46) into (39), I_2 can be written as

$$I_2 = \ln(2s^2) + \frac{1}{s^2} E_{X^*} \left\{ \frac{1}{\sqrt{2\pi q}} \frac{1}{\sqrt{2\pi p}} \int_{-\infty}^{\infty} e^{-\frac{(y_B - H_B x)^2}{2q}} \int_{-\infty}^{\infty} e^{-\frac{t^2}{2p}} \left| \left(1 - \mu \frac{H_E}{H_B} \right) y_B - \mu t \right| dt dy_B \right\} \tag{47}$$

Then I_2 can be upper-bounded by

$$\begin{aligned}
 I_2 & \leq \ln(2s^2) + \frac{|1 - \mu \frac{H_E}{H_B}|}{s^2} E_{X^*} \left\{ \frac{2}{\sqrt{2\pi q}} + H_B x \right\} + \frac{2|\mu|}{s^2} E_{X^*} \left\{ \frac{1}{\sqrt{2\pi p}} \right\} \\
 & \leq \ln(2s^2) + \frac{|1 - \mu \frac{H_E}{H_B}|}{s^2} H_B \xi P + \frac{2|1 - \mu \frac{H_E}{H_B}|}{s^2} E_{X^*} \left\{ \frac{1}{\sqrt{2\pi q}} \right\} + \frac{2|\mu|}{s^2} E_{X^*} \left\{ \frac{1}{\sqrt{2\pi p}} \right\} \\
 & = \ln(2s^2) + \frac{2}{s^2} \underbrace{\left[\left| 1 - \mu \frac{H_E}{H_B} \right| \left(\sqrt{\frac{3}{\pi^2 H_B \varsigma_1^2 \sigma_B^2 \xi P} + \frac{H_B \xi P}{2}} \right) + |\mu| \sqrt{\frac{3}{\pi^2 \xi P \left(\frac{H_E^2}{H_B^2} \varsigma_1^2 \sigma_B^2 + H_E \varsigma_2^2 \sigma_E^2 \right)}} \right]}_{I_3}
 \end{aligned} \tag{48}$$

Case1: when $\mu < 0$, I_3 is given by

$$\begin{aligned}
 I_3 &= -\mu \left[\frac{H_E}{H_B} \left(\sqrt{\frac{3}{\pi^2 H_B \varsigma_1^2 \sigma_B^2 \xi P} + \frac{H_B \xi P}{2}} \right) + \sqrt{\frac{3}{\pi^2 \xi P \left(\frac{H_E^2}{H_B} \varsigma_1^2 \sigma_B^2 + H_E \varsigma_2^2 \sigma_E^2 \right)}} \right] \\
 &\quad + \left(\sqrt{\frac{3}{\pi^2 H_B \varsigma_1^2 \sigma_B^2 \xi P} + \frac{H_B \xi P}{2}} \right) \\
 &\geq \sqrt{\frac{3}{\pi^2 H_B \varsigma_1^2 \sigma_B^2 \xi P} + \frac{H_B \xi P}{2}}
 \end{aligned} \tag{49}$$

Case2: when $0 \leq \mu \leq H_B/H_E$, I_3 is given by

$$\begin{aligned}
 I_3 &= \mu \left[\sqrt{\frac{3}{\pi^2 \xi P \left(\frac{H_E^2}{H_B} \varsigma_1^2 \sigma_B^2 + H_E \varsigma_2^2 \sigma_E^2 \right)}} - \frac{H_E}{H_B} \left(\sqrt{\frac{3}{\pi^2 H_B \varsigma_1^2 \sigma_B^2 \xi P} + \frac{H_B \xi P}{2}} \right) \right] \\
 &\quad + \left(\sqrt{\frac{3}{\pi^2 H_B \varsigma_1^2 \sigma_B^2 \xi P} + \frac{H_B \xi P}{2}} \right)
 \end{aligned} \tag{50}$$

So I_3 can be lower-bounded by

$$I_3 \geq \begin{cases} \sqrt{\frac{3}{\pi^2 H_B \varsigma_1^2 \sigma_B^2 \xi P} + \frac{H_B \xi P}{2}}, & \text{if } \sqrt{\frac{3}{\pi^2 \xi P \left(\frac{H_E^2}{H_B} \varsigma_1^2 \sigma_B^2 + H_E \varsigma_2^2 \sigma_E^2 \right)}} \\ \geq \frac{H_E}{H_B} \left(\sqrt{\frac{3}{\pi^2 H_B \varsigma_1^2 \sigma_B^2 \xi P} + \frac{H_B \xi P}{2}} \right) \\ \frac{H_E}{H_E} \sqrt{\frac{3}{\pi^2 \xi P \left(\frac{H_E^2}{H_B} \varsigma_1^2 \sigma_B^2 + H_E \varsigma_2^2 \sigma_E^2 \right)}}, & \text{if } \sqrt{\frac{3}{\pi^2 \xi P \left(\frac{H_E^2}{H_B} \varsigma_1^2 \sigma_B^2 + H_E \varsigma_2^2 \sigma_E^2 \right)}} \\ < \frac{H_E}{H_B} \left(\sqrt{\frac{3}{\pi^2 H_B \varsigma_1^2 \sigma_B^2 \xi P} + \frac{H_B \xi P}{2}} \right) \end{cases} \tag{51}$$

Case3: when $\mu > H_B/H_E$, I_3 is given by

$$\begin{aligned}
 I_3 &= \mu \left[\frac{H_E}{H_B} \left(\sqrt{\frac{3}{\pi^2 H_B \varsigma_1^2 \sigma_B^2 \xi P} + \frac{H_B \xi P}{2}} \right) + \sqrt{\frac{3}{\pi^2 \xi P \left(\frac{H_E^2}{H_B} \varsigma_1^2 \sigma_B^2 + H_E \varsigma_2^2 \sigma_E^2 \right)}} \right] \\
 &\quad - \left(\sqrt{\frac{3}{\pi^2 H_B \varsigma_1^2 \sigma_B^2 \xi P} + \frac{H_B \xi P}{2}} \right) \geq \frac{H_E}{H_E} \sqrt{\frac{3}{\pi^2 \xi P \left(\frac{H_E^2}{H_B} \varsigma_1^2 \sigma_B^2 + H_E \varsigma_2^2 \sigma_E^2 \right)}}
 \end{aligned} \tag{52}$$

From three cases, I_3 can be expressed as

$$I_3 \geq \begin{cases} \sqrt{\frac{3}{\pi^2 H_B \varsigma_1^2 \sigma_B^2 \xi P} + \frac{H_B \xi P}{2}}, & \text{if } \sqrt{\frac{3}{\pi^2 \xi P \left(\frac{H_E^2}{H_B} \varsigma_1^2 \sigma_B^2 + H_E \varsigma_2^2 \sigma_E^2 \right)}} \\ \geq \frac{H_E}{H_B} \left(\sqrt{\frac{3}{\pi^2 H_B \varsigma_1^2 \sigma_B^2 \xi P} + \frac{H_B \xi P}{2}} \right) \\ \frac{H_B}{H_E} \sqrt{\frac{3}{\pi^2 \xi P \left(\frac{H_E^2}{H_B} \varsigma_1^2 \sigma_B^2 + H_E \varsigma_2^2 \sigma_E^2 \right)}}, & \text{if } \sqrt{\frac{3}{\pi^2 \xi P \left(\frac{H_E^2}{H_B} \varsigma_1^2 \sigma_B^2 + H_E \varsigma_2^2 \sigma_E^2 \right)}} \\ < \frac{H_E}{H_B} \left(\sqrt{\frac{3}{\pi^2 H_B \varsigma_1^2 \sigma_B^2 \xi P} + \frac{H_B \xi P}{2}} \right) \end{cases} \quad (53)$$

Substituting (53) into (48) I_2 can be written as

$$I_2 \leq \begin{cases} \ln \left[4e \left(\sqrt{\frac{3}{\pi^2 H_B \varsigma_1^2 \sigma_B^2 \xi P} + \frac{H_B \xi P}{2}} \right) \right], & \text{if } \sqrt{\frac{3}{\pi^2 \xi P \left(\frac{H_E^2}{H_B} \varsigma_1^2 \sigma_B^2 + H_E \varsigma_2^2 \sigma_E^2 \right)}} \\ \geq \frac{H_E}{H_B} \left(\sqrt{\frac{3}{\pi^2 H_B \varsigma_1^2 \sigma_B^2 \xi P} + \frac{H_B \xi P}{2}} \right) \\ \ln \left[4e \frac{H_B}{H_E} \sqrt{\frac{3}{\pi^2 \xi P \left(\frac{H_E^2}{H_B} \varsigma_1^2 \sigma_B^2 + H_E \varsigma_2^2 \sigma_E^2 \right)}} \right], & \text{if } \sqrt{\frac{3}{\pi^2 \xi P \left(\frac{H_E^2}{H_B} \varsigma_1^2 \sigma_B^2 + H_E \varsigma_2^2 \sigma_E^2 \right)}} \\ < \frac{H_E}{H_B} \left(\sqrt{\frac{3}{\pi^2 H_B \varsigma_1^2 \sigma_B^2 \xi P} + \frac{H_B \xi P}{2}} \right) \end{cases} \quad (54)$$

Then substituting (44) and (54) into (39), the secrecy capacity (15) can be derived.

References

1. Andrews, J.G., Buzzi, S., Choi, W., Hanly, S.V.: What will 5G be. *IEEE J. Sel. Areas Commun.* **32**(3), 1065–1082 (2014)
2. Komine, T., Nakagawa, M.: Fundamental analysis for visible-light communication system using LED lights. *IEEE Trans. Consum. Electron.* **50**(1), 100–107 (2004)
3. Karunatilaka, D., Zafar, F., Kalavally, V., Parthiban, R.: LED based indoor visible light communications: state of the art. *IEEE Commun. Surv. Tut.* **17**(3), 1649–1678 (2015)
4. Shannon, C.E.: Communication theory of secrecy systems. *Bell Syst. Tech. J.* **28**(4), 656–715 (1949)
5. Wyner, D.: The wire-tap channel. *Bell Syst. Tech. J.* **54**, 1355–1387 (1975)
6. Lapidath, A., Moser, S.M.: Capacity bounds via duality with applications to multiple-antenna systems on flat fading channels. *IEEE Trans. Inf. Theory* **49**(10), 2426–2467 (2003)
7. Lapidath, A., Moser, S.M., Wigger, M.A.: On the capacity of free-space optical intensity channels. *IEEE Trans. Inf. Theory* **55**(10), 4449–4461 (2009)

8. Mostafa, A., Lampe, L.: Physical-layer security for MISO visible light communication channels. *IEEE J. Sel. Areas Commun.* **33**(9), 1806–1818 (2015)
9. Wang, J.-Y., Dai, J., Guan, R., Jia, L., Wang, Y., Chen, M.: On the channel capacity and receiver deployment optimization for multi-input multi-output visible light communications. *Opt. Exp.* **24**(12), 13060–13074 (2016)
10. Wang, J.-Y., Liu, C., Wang, J., Wu, Y., Lin, M., Cheng, J.: Physical layer security for indoor visible light communications: secrecy capacity analysis. *IEEE Trans. Commun.* **66**(12), 6423–6436 (2018)
11. Moser, S.M.: Capacity results of an optical intensity channel with input dependent Gaussian noise. *IEEE Trans. Inf. Theory* **58**(1), 207–223 (2012)
12. Cover, T., Thomas, J.: *Elements of Information Theory*, 2nd edn. Wiley, Hoboken (2006)
13. Csiszar, I., Korner, J.: *Information Theory: Coding Theorems for Discrete Memoryless Systems*. Academic, New York (1981)